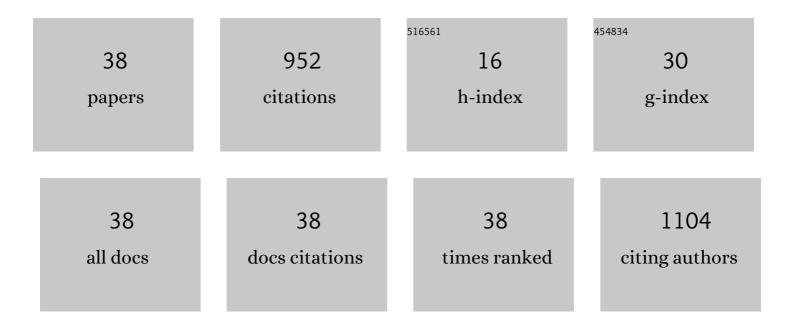
Renuka Sriram

List of Publications by Year in descending order

Source: https://exaly.com/author-pdf/8858833/publications.pdf Version: 2024-02-01



#	Article	IF	CITATIONS
1	Clinical translation of hyperpolarized ¹³ C pyruvate and urea MRI for simultaneous metabolic and perfusion imaging. Magnetic Resonance in Medicine, 2022, 87, 138-149.	1.9	23
2	In Vivo Profiling with ¹⁸ F-YJH08 Reveals Diverse Tissue Patterns of Antagonist/Glucocorticoid Receptor Interactions. Molecular Pharmaceutics, 2022, 19, 704-709.	2.3	2
3	CUB Domain-Containing Protein 1 (CDCP1) Is a Target for Radioligand Therapy in Castration-Resistant Prostate Cancer, including PSMA Null Disease. Clinical Cancer Research, 2022, 28, 3066-3075.	3.2	10
4	Molecular Imaging of Prostate Cancer Targeting CD46 Using ImmunoPET. Clinical Cancer Research, 2021, 27, 1305-1315.	3.2	18
5	Using Hyperpolarized NMR to Understand Biochemistry from Cells to Humans. , 2021, , 123-149.		1
6	Modeling hyperpolarized lactate signal dynamics in cells, patientâ€derived tissue slice cultures and murine models. NMR in Biomedicine, 2021, 34, e4467.	1.6	5
7	Resistance to Androgen Deprivation Leads to Altered Metabolism in Human and Murine Prostate Cancer Cell and Tumor Models. Metabolites, 2021, 11, 139.	1.3	13
8	Deuterium Metabolic Imaging-Rediscovery of a Spectroscopic Tool. Metabolites, 2021, 11, .	1.3	0
9	HP experimental methods: cells and animals. Advances in Magnetic Resonance Technology and Applications, 2021, 3, 75-91.	0.0	0
10	Deuterium Metabolic Imaging—Rediscovery of a Spectroscopic Tool. Metabolites, 2021, 11, 570.	1.3	12
11	Simultaneous Metabolic and Perfusion Imaging Using Hyperpolarized 13C MRI Can Evaluate Early and Dose-Dependent Response to Radiation Therapy in a Prostate Cancer Mouse Model. International Journal of Radiation Oncology Biology Physics, 2020, 107, 887-896.	0.4	18
12	Elevated Tumor Lactate and Efflux in High-grade Prostate Cancer demonstrated by Hyperpolarized 13C Magnetic Resonance Spectroscopy of Prostate Tissue Slice Cultures. Cancers, 2020, 12, 537.	1.7	14
13	Sensing Living Bacteria <i>in Vivo</i> Using <scp>d</scp> -Alanine-Derived ¹¹ C Radiotracers. ACS Central Science, 2020, 6, 155-165.	5.3	48
14	Assessing highâ€intensity focused ultrasound treatment of prostate cancer with hyperpolarized ¹³ C dualâ€agent imaging of metabolism and perfusion. NMR in Biomedicine, 2019, 32, e3962.	1.6	10
15	Amino Acidâ€Đerived Sensors for Specific Zn ²⁺ Detection Using Hyperpolarized ¹³ C Magnetic Resonance Spectroscopy. Chemistry - A European Journal, 2019, 25, 11842-11846.	1.7	8
16	First hyperpolarized [2-13C]pyruvate MR studies of human brain metabolism. Journal of Magnetic Resonance, 2019, 309, 106617.	1.2	63
17	Using bidirectional chemical exchange for improved hyperpolarized [¹³ C]bicarbonate pH imaging. Magnetic Resonance in Medicine, 2019, 82, 959-972.	1.9	8
18	The Role of Lactate Metabolism in Prostate Cancer Progression and Metastases Revealed by Dual-Agent Hyperpolarized 13C MRSI. Cancers, 2019, 11, 257.	1.7	41

Renuka Sriram

#	Article	IF	CITATIONS
19	NMR quantification of lactate production and efflux and glutamate fractional enrichment in living human prostate biopsies cultured with [1,6â€< sup>13C ₂]glucose. Magnetic Resonance in Medicine, 2019, 82, 566-576.	1.9	7
20	Measuring Dynamic Changes in the Labile Iron Pool in Vivo with a Reactivity-Based Probe for Positron Emission Tomography. ACS Central Science, 2019, 5, 727-736.	5.3	38
21	Hyperpolarized <i>in vivo</i> pH imaging reveals grade-dependent acidification in prostate cancer. Oncotarget, 2019, 10, 6096-6110.	0.8	16
22	Detection of Bacteria-Specific Metabolism Using Hyperpolarized [2- ¹³ C]Pyruvate. ACS Infectious Diseases, 2018, 4, 797-805.	1.8	13
23	[¹¹ C]Para-Aminobenzoic Acid: A Positron Emission Tomography Tracer Targeting Bacteria-Specific Metabolism. ACS Infectious Diseases, 2018, 4, 1067-1072.	1.8	54
24	Non-Invasive Assessment of Lactate Production and Compartmentalization in Renal Cell Carcinomas Using Hyperpolarized 13C Pyruvate MRI. Cancers, 2018, 10, 313.	1.7	22
25	Imaging glutathione depletion in the rat brain using ascorbate-derived hyperpolarized MR and PET probes. Scientific Reports, 2018, 8, 7928.	1.6	20
26	Molecular detection of inflammation in cell models using hyperpolarized ¹³ C-pyruvate. Theranostics, 2018, 8, 3400-3407.	4.6	19
27	Measuring glucocorticoid receptor expression <i>in vivo</i> with PET. Oncotarget, 2018, 9, 20399-20408.	0.8	8
28	Assessing Prostate Cancer Aggressiveness with Hyperpolarized Dual-Agent 3D Dynamic Imaging of Metabolism and Perfusion. Cancer Research, 2017, 77, 3207-3216.	0.4	60
29	Imaging Active Infection in vivo Using D-Amino Acid Derived PET Radiotracers. Scientific Reports, 2017, 7, 7903.	1.6	58
30	Monitoring acute metabolic changes in the liver and kidneys induced by fructose and glucose using hyperpolarized [2â€ ¹³ C]dihydroxyacetone. Magnetic Resonance in Medicine, 2017, 77, 65-73.	1.9	28
31	Separation of extra- and intracellular metabolites using hyperpolarized 13C diffusion weighted MR. Journal of Magnetic Resonance, 2016, 270, 115-123.	1.2	19
32	Non-Invasive Differentiation of Benign Renal Tumors from Clear Cell Renal Cell Carcinomas Using Clinically Translatable Hyperpolarized 13C Pyruvate Magnetic Resonance. Tomography, 2016, 2, 35-42.	0.8	26
33	Metabolic response of prostate cancer to nicotinamide phophoribosyltransferase inhibition in a hyperpolarized MR/PET compatible bioreactor. Prostate, 2015, 75, 1601-1609.	1.2	30
34	Realâ€ŧime measurement of hyperpolarized lactate production and efflux as a biomarker of tumor aggressiveness in an MR compatible 3D cell culture bioreactor. NMR in Biomedicine, 2015, 28, 1141-1149.	1.6	43
35	Dynamic UltraFast 2D EXchange SpectroscopY (UF-EXSY) of hyperpolarized substrates. Journal of Magnetic Resonance, 2015, 257, 102-109.	1.2	9
36	Hyperpolarized 13C-Pyruvate Magnetic Resonance Reveals Rapid Lactate Export in Metastatic Renal Cell Carcinomas. Cancer Research, 2013, 73, 529-538.	0.4	95

#	Article	IF	CITATIONS
37	Metabolic Reprogramming and Validation of Hyperpolarized ¹³ C Lactate as a Prostate Cancer Biomarker Using a Human Prostate Tissue Slice Culture Bioreactor. Prostate, 2013, 73, 1171-1181.	1.2	93
38	Defining the Magnetic Resonance Features of Renal Lesions and Their Response to Everolimus in a Transgenic Mouse Model of Tuberous Sclerosis Complex. Frontiers in Oncology, 0, 12, .	1.3	0